

Impacts of biogenic isoprene emission on ozone air quality in the Seoul metropolitan area

Kwang-Yeon Lee ^a, Kyung-Hwan Kwak ^a, Young-Hee Ryu ^{a,b}, Sang-Hyun Lee ^c,
Jong-Jin Baik ^{a,*}

^a School of Earth and Environmental Sciences, Seoul National University, Seoul 151-742, Republic of Korea

^b Department of Civil and Environmental Engineering, Princeton University, NJ 08544, USA

^c Department of Atmospheric Science, Kongju National University, Gongju 314-701, Republic of Korea



HIGHLIGHTS

- The impacts of biogenic isoprene emission on O₃ air quality are numerically examined.
- The increase in O₃ concentration can be 37 ppb due to the biogenic isoprene emission.
- The increase is largely caused by the isoprene emission from the surrounding region.
- HCHO, CCHO, and MPAN transport by local circulations worsens urban O₃ air quality.

ARTICLE INFO

Article history:

Received 4 March 2014

Received in revised form

17 July 2014

Accepted 19 July 2014

Available online 19 July 2014

Keywords:

Biogenic isoprene emission

Isoprene oxidation products

Ozone air quality

Seoul

WRF model

CMAQ modeling system

ABSTRACT

The impacts of biogenic isoprene emission on ozone (O₃) air quality during an episode under weak synoptic forcing in the Seoul metropolitan area (SMA), Republic of Korea, are investigated using the Community Multiscale Air Quality (CMAQ) modeling system coupled with the Weather Research and Forecasting (WRF) model. Simulations with different biogenic isoprene emission scenarios show that the impact of biogenic isoprene emission on the daily maximum O₃ concentration is as high as 37 ppb in the Seoul region. The O₃ concentration in the Seoul region is significantly increased by the biogenic isoprene emission from the surrounding region compared to that from within the Seoul region. In addition, the gas-phase chemistry is found to be the most important process for O₃ concentration in the Seoul region in the presence of the biogenic isoprene emission from the surrounding region. While isoprene is not enough to influence O₃ concentration directly due to its short lifetime, the transport of isoprene oxidation products plays a crucial role in increasing O₃ concentration in the Seoul region. Through the process analysis, peroxy methacryloyl nitrate (MPAN) as well as formaldehyde (HCHO) and acetaldehyde (CCHO) is also identified as the important precursor that links biogenic isoprene emission from the surrounding region to O₃ concentration in the Seoul region. After transported by daytime local circulations, the chemistry of isoprene oxidation products contributes to O₃ formation in the Seoul region.

© 2014 Elsevier Ltd. All rights reserved.

1. Introduction

Ozone (O₃) is one of the most harmful pollutants existing in the urban atmosphere. Long-term exposure to O₃ reduces lung function and increases the risk of asthma in children and nonsmoking adults (McDonnell et al., 1999; WHO, 2003; Lin et al., 2008). In addition, O₃ damages urban trees (Trahern and Peterson, 2007) and degrades rubber and textiles (Lee et al., 1996). O₃ is produced by

photochemical reactions in relation to NO_x (=NO + NO₂) and volatile organic compounds (VOCs) in urban areas (Haagen-Smit and Fox, 1954). In general, O₃ concentration in urban areas is more sensitive to VOCs concentration than NO_x concentration (Milford et al., 1989, 1994; Sillman, 1999). Over the past few decades, biogenic VOCs as well as anthropogenic VOCs have been recognized as important sources for O₃ formation in urban areas (Chameides et al., 1988).

Isoprene is the most influential species for O₃ formation among biogenic VOCs. The effects of isoprene on O₃ concentration in urban areas have been investigated by many researchers. The contribution of isoprene to O₃ formation becomes significant in a range up to 75% (e.g., Duane et al., 2002) under high air temperature, strong

* Corresponding author.

E-mail address: jbaik@snu.ac.kr (J.-J. Baik).

solar radiation, and high NO_x level. The effects of isoprene on O_3 concentration are evident and consistent for cities around the world, for example, Vancouver, Canada (Biesenthal et al., 1997), Kaohsiung, Taiwan (Chang et al., 2005), Houston, USA (Li et al., 2007), and Beijing, China (Duan et al., 2008).

The Seoul metropolitan area (SMA) that consists of Seoul, Incheon, and parts of Gyeonggi province is the largest urban area in Korea (population of approximately 22 million). Seoul is surrounded by several mountains to the east, south, and north, and is open to the west. O_3 episodes in the SMA have been studied mostly in association with meteorological aspects. It is known that high O_3 concentration occurs when the sea/land breeze is well developed under weak synoptic forcing regardless of prevailing wind direction (Ghim et al., 2001). It is also known that the recirculation of O_3 precursors has a significant influence on O_3 concentration. Jeon et al. (2012) showed that the recirculation leads to the increase in O_3 concentration by 10.9 ppb when the average NO_x and VOCs concentrations increase by 2.9% and 19.7%, respectively, in an episode of July 2007. Shin et al. (2013) calculated the contributions of VOCs to O_3 formation using four-year observation data and showed the greatest contribution of aromatic compounds.

Despite large biogenic VOCs emissions around the SMA, the impacts of biogenic emissions on O_3 concentration in the area are still poorly understood. Recently, Ryu et al. (2013) examined the impacts of urban land-surface forcing on O_3 concentration in the SMA under weak synoptic forcing using the Community Multiscale Air Quality (CMAQ) modeling system coupled with the Weather Research and Forecasting (WRF) model. They found that one of the important phenomena responsible for increasing O_3 concentration in the presence of urban land-surface forcing is the urban breeze circulation that transports air masses from the mountain area to the urban area in the afternoon. The air masses were found to be characterized by low NO_x and high VOCs levels, resulting in long OH chain lengths. This implies that biogenic isoprene plays a critical role in increasing O_3 concentration in the SMA.

In this study, the impacts of biogenic isoprene emission on O_3 concentration in the SMA are examined using the CMAQ modeling system coupled with the WRF model. To understand how biogenic isoprene emission affects O_3 concentration in the SMA, sensitivity simulations using different isoprene emission scenarios are performed, and then simulation and analysis results are presented and discussed. We focus particularly on pathways involved between biogenic isoprene emission and O_3 concentration.

2. Methodology

2.1. Meteorology model

The WRF model version 3.2 (Skamarock et al., 2008) is used to provide the meteorological inputs for the CMAQ modeling system. For a better representation of urban surface processes, the Seoul National University Urban Canopy Model (SNUUCM) (Ryu et al., 2011) is coupled with the WRF model. Four model domains with horizontal grid sizes of 27, 9, 3, and 1 km are considered. The number of vertical layers is 43, and 16 vertical layers exist below a 2-km height. The lowest vertical grid size is ~35 m. The model is integrated for 72 h from 0000 UTC on 22 June 2010. The National Centers for Environmental Prediction (NCEP) final analysis data are used for initial and boundary conditions. Other experimental setups and the case selected are the same as those in Ryu and Baik (2013).

2.2. Air quality modeling system

The CMAQ modeling system version 4.7.1 (Byun and Schere, 2006) is used in this study. In the air quality simulations, three

domains with horizontal grid sizes of 9, 3, and 1 km are considered (Fig. 1a). The default concentration profiles in the CMAQ modeling system are used as initial and boundary conditions in the outermost domain. In the inner two domains, the simulation results in their outer domains are used as boundary conditions. The 29 vertical layers are used in this study, and the lowest 22 layers are the same as those used in the WRF simulation. The Statewide Air Pollution Research Center version 99 (SAPRC-99) chemical mechanism (Carter, 2000) that contains 77 chemical species and 224 chemical reactions and the fifth-generation model CMAQ aerosol module (Foley et al., 2010) are used. The model is integrated for 72 h from 0000 UTC on 22 June 2010, and the results of 0600–2000 LT on 24 June (i.e., from 2100 UTC on 23 June to 1100 UTC on 24 June) are analyzed.

Hourly anthropogenic emission data are estimated for all domains using the Sparse Matrix Operator Kernel Emissions (SMOKE) system (Houyoux et al., 2000). The Model of Emissions of Gases and Aerosols from Nature (MEGAN) (Guenther et al., 2006) is used to estimate hourly biogenic emissions. For example, biogenic isoprene emission is estimated depending on the land-use/land-cover categories (Fig. 1b) and atmospheric conditions. In the SMA, the biogenic isoprene emission rates in forest areas are generally much higher than those in urban areas (Fig. 1c).

To elucidate the impacts of biogenic isoprene emission on O_3 concentration, three additional simulations are performed where biogenic isoprene emissions are removed from different regions: the Seoul region (hereafter, the OUT simulation) (Fig. 1d), outside of the Seoul region (hereafter, the IN simulation) (Fig. 1e), or over the entire domain (hereafter, the NONE simulation) (Fig. 1f). Note that anthropogenic isoprene emission mainly from mobile sources is not totally negligible particularly in urban areas (Park et al., 2011). Except for biogenic isoprene emission, other emissions including the anthropogenic isoprene emission in the additional simulations are set to be identical to those in the control simulation (hereafter, the ALL simulation).

3. Results and discussion

3.1. Model validation

The air quality model is validated for the O_3 concentration in the ALL simulation against observation data measured by UV absorption O_3 analyzers at five air quality monitoring stations. The measured O_3 concentrations are given in parts per billion (ppb) by rounding off to the nearest whole number. The five monitoring stations are located in urban areas in the eastern part of Seoul (Gangdong-gu, Fig. 2a) and in satellite cities located in the southeast (Sunnam, Fig. 2b), the east (Guri, Fig. 2c), the north (Uijeongbu, Fig. 2d), and the south (Anyang, Fig. 2e). These monitoring stations are close to the border between Seoul and Gyeonggi province (Fig. 1f). The diurnal variations of simulated and observed O_3 concentrations on 24 June 2010 are compared (Fig. 2). In the daytime, the maximum O_3 concentrations are slightly underestimated at Guri and Anyang stations and overestimated at Gangdong-gu, Sunnam, and Uijeongbu stations. Despite the site variability, the CMAQ modeling system generally well reproduces the diurnal patterns of O_3 concentration.

3.2. Control simulation

Fig. 3 shows the near-surface O_3 concentration and horizontal wind fields in the SMA at 1200, 1400, 1600, and 1800 LT. The near-surface concentration and wind vector are calculated at the lowest model level. At 1200 LT, the O_3 concentration rapidly increases particularly in the eastern part of the SMA where biogenic

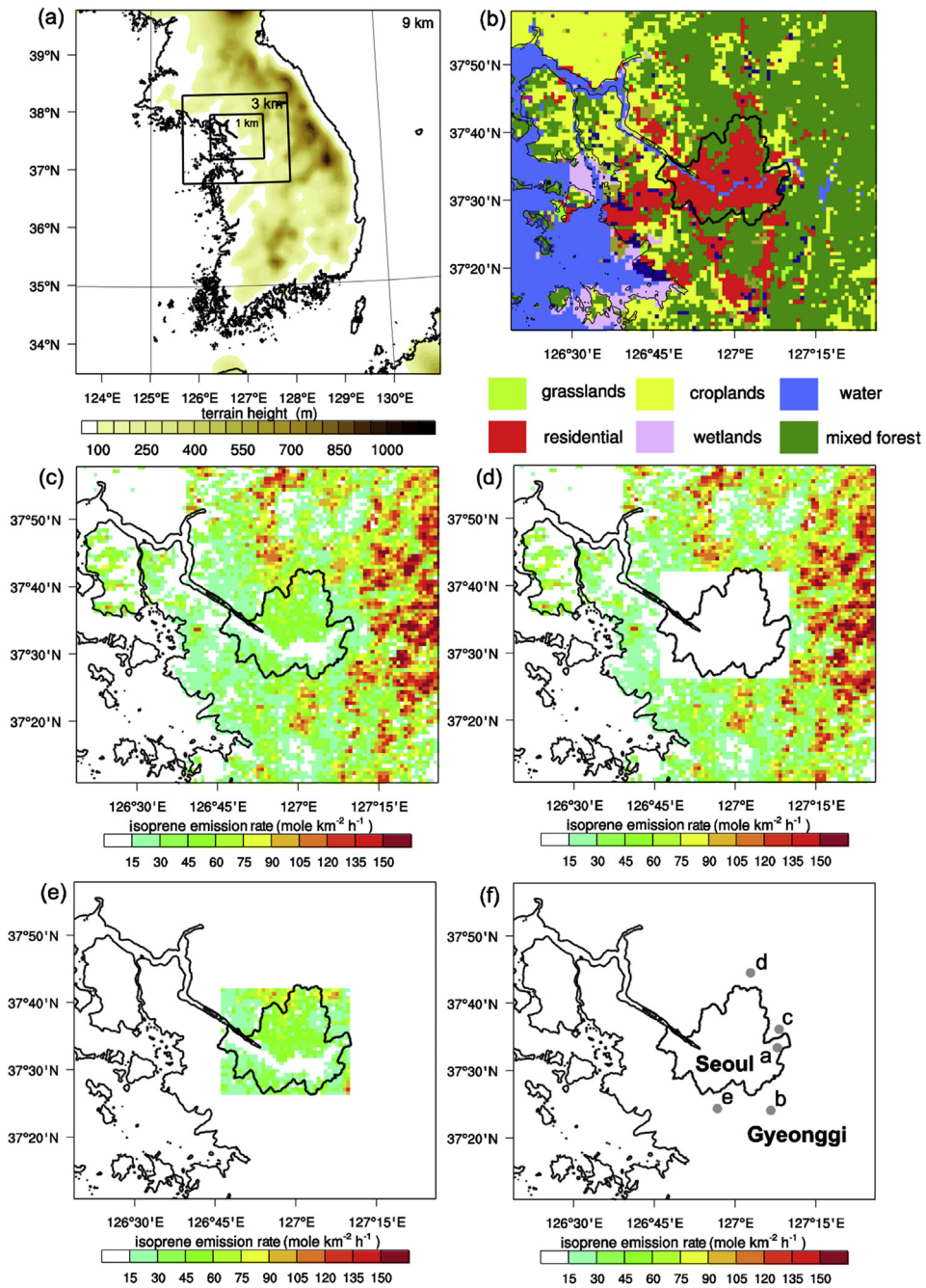


Fig. 1. (a) CMAQ simulation domains with terrain height and (b) land-use/land-cover in the innermost domain. Biogenic isoprene emission rates in the (c) ALL, (d) OUT, (e) IN, and (f) NONE simulations at 1500 LT on 24 June 2010 in the innermost domain. Fig. 1a–c is after Fig. 1a, b, and d of Ryu et al. (2013). The locations of five air quality monitoring stations (a–e) selected for the model validation are indicated by gray circles in Fig. 1f.

emissions are high. At 1400 LT, the O_3 concentration in the Seoul region increases in relation to the transport from the surrounding region by daytime local circulations as well as the photochemical production. At 1600 LT when the near-surface wind apparently converges into the Seoul region, the high O_3 concentration extends toward the Seoul region particularly in the northern part of Seoul. At 1800 LT, the O_3 concentration still remains high as the westerly wind penetrates into the SMA to the eastside of Seoul region.

The temporal variations of the atmospheric boundary layer-averaged O_3 and isoprene concentrations in the Seoul region from 0600 to 2000 LT are shown in Fig. 4a and c, respectively. In the ALL simulation, the O_3 concentration continuously increases and

reaches a daily maximum of 82 ppb at 1800 LT. On the other hand, the isoprene concentration reaches a daily maximum at 0900 LT and a second maximum at 1900 LT. In the afternoon, isoprene is rapidly oxidized and mixed in the deepened atmospheric boundary layer, resulting in local minimum of its concentration at 1500 LT.

3.3. Impacts of biogenic isoprene emission

To examine the impacts of biogenic isoprene emission on O_3 concentration in the SMA, the O_3 and isoprene concentrations in the OUT, IN, and NONE simulations are compared to those in the ALL simulation (Fig. 4). The daily maximum O_3 concentrations in

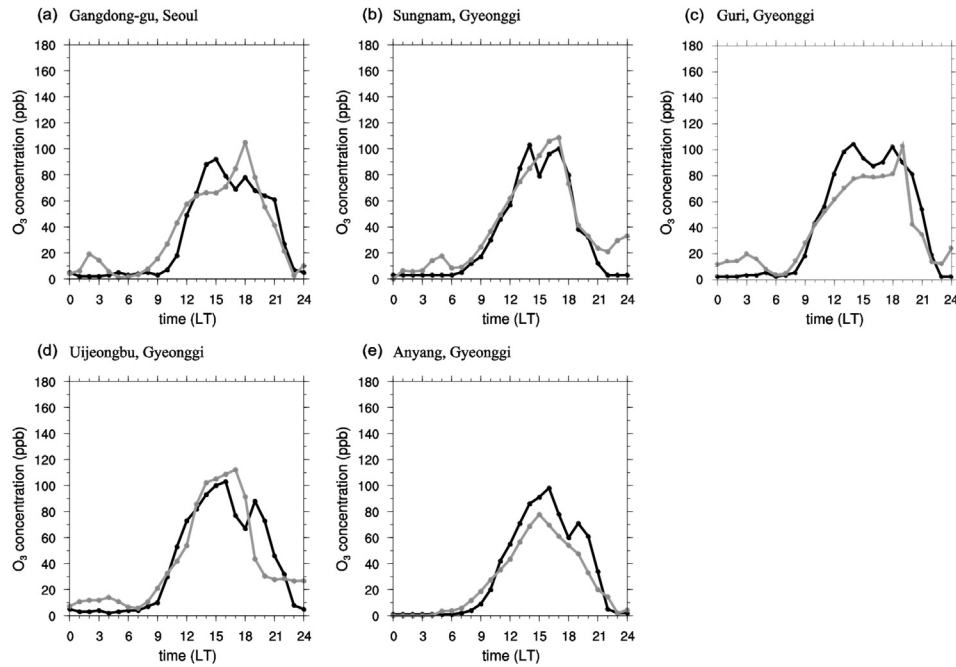


Fig. 2. Diurnal variations of simulated (gray line) and observed (black line) O_3 concentrations near surfaces on 24 June 2010 at five air quality monitoring stations that are located in (a) Gangdong-gu, Seoul, (b) Sungnam, Gyeonggi, (c) Guri, Gyeonggi, (d) Uijeongbu, Gyeonggi, and (e) Anyang, Gyeonggi.

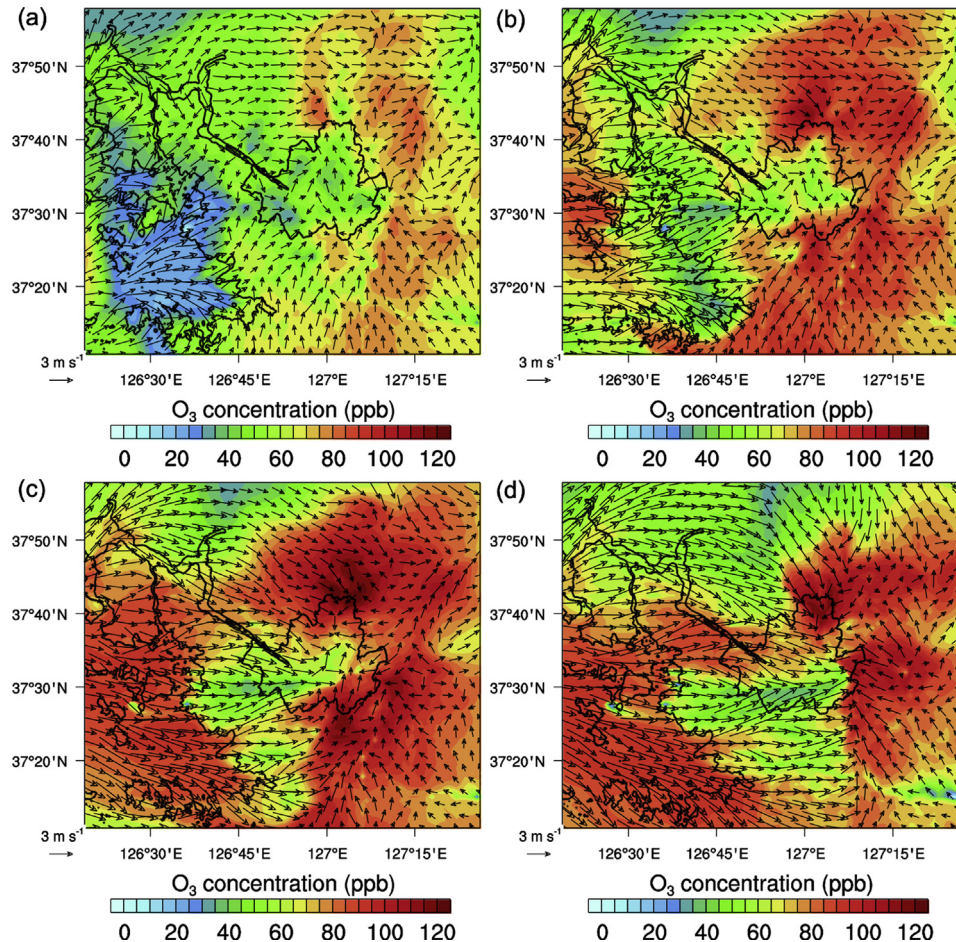


Fig. 3. Near-surface O_3 concentration and horizontal wind fields at (a) 1200, (b) 1400, (c) 1600, and (d) 1800 LT in the ALL simulation.

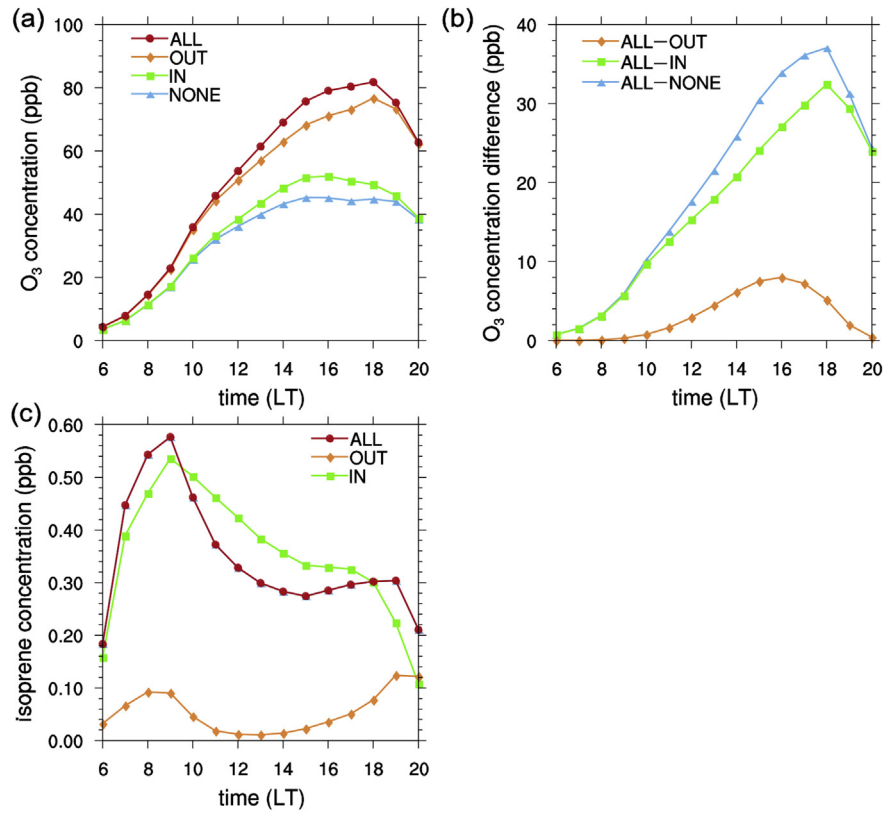


Fig. 4. Temporal variations of the atmospheric boundary layer-averaged (a) O₃ and (c) isoprene concentrations in the Seoul region from 0600 to 2000 LT in the ALL, OUT, IN, and NONE simulations. (b) Temporal variations of the atmospheric boundary layer-averaged differences in O₃ concentration between the ALL simulation and the OUT, IN, or NONE simulation in the Seoul region.

the OUT, IN, and NONE simulations are 78 ppb at 1800 LT, 52 ppb at 1500 LT, and 45 ppb at 1600 LT, respectively. This implies that the increase and late appearance of daily maximum O₃ concentration in the ALL simulation are mostly attributed to the influence of biogenic isoprene emission from the surrounding region. The influence is the largest at 1800 LT as shown by the difference in O₃ concentration between the ALL simulation and the IN or NONE simulation (Fig. 4b). On the other hand, the difference in O₃ concentration between the ALL and OUT simulations shows that the influence of biogenic isoprene emission from within the Seoul region is maximized at 1600 LT. In the daytime, the difference in O₃ concentration between the ALL and IN simulations is consistently larger than that between the ALL and OUT simulations. This implies that the biogenic isoprene emission from the surrounding region has a greater influence on the O₃ concentration in the Seoul region than that from within the Seoul region. The isoprene concentration in the OUT simulation is significantly lower than that in the ALL and IN simulations due to a short lifetime of isoprene not enough to be transported into the Seoul region. The daily maximum isoprene concentrations in the IN and OUT simulations appear at 0900 and 1900 LT, respectively. In the ALL simulation, the sources responsible for the daily and secondary maxima of isoprene concentration are thought to be different from each other, which can be the isoprene emission from within the Seoul region and that from the surrounding region, respectively. The higher isoprene concentration in the IN simulation than in the ALL simulation from 1000 to 1700 LT is possibly due to the lower concentrations of OH radical in the IN simulation than in the ALL simulation. In opposition to the O₃ concentration, the higher isoprene concentration in the IN simulation than in the OUT simulation in the daytime implies that the

direct impact of biogenic isoprene emission on the O₃ concentration is spatially rather limited within source areas.

Fig. 5a–c shows the near-surface O₃ concentration and horizontal wind fields at 1600 LT in the OUT, IN, and NONE simulations. At this time, daytime local circulations become apparent and dominate pollutant transport over the SMA. The O₃ concentration in the surrounding region is generally higher than that in the Seoul region in these simulations. In the OUT and IN simulations as well as in the ALL simulation (Fig. 3c), the highest O₃ concentration in the SMA appears on the north side of Seoul region where mountains are located. Note that the highest O₃ concentration in the SMA in the NONE simulation appears to the far east of the Seoul region. As shown in Fig. 4, the O₃ concentration in the simulations with biogenic isoprene emission from the surrounding region (i.e., ALL and OUT simulations) is generally higher than that in the simulations without it (i.e., IN and NONE simulations). Therefore, it is clear that the increase in O₃ concentration in the Seoul region is not only due to photochemical production but also due to transport of air masses as demonstrated by Ryu et al. (2013). The ratios of the difference in O₃ concentration between the ALL and IN simulations to the O₃ concentration in the ALL simulation at 1600 LT are shown in Fig. 5d. The ratio is obviously over 30% in most parts of the SMA except for the eastern part. The influence of biogenic isoprene emission on O₃ concentration in the Seoul region is possibly due to the transport by the daytime local circulations. Although the O₃ concentration is high in the eastern part of the SMA, the influence from the eastern part is not seen to be significant.

To evaluate how the biogenic isoprene emission from the surrounding region affects the O₃ concentration in the Seoul region, an integrated process rate (IPR) analysis (Jeffries and Tonnesen, 1994)

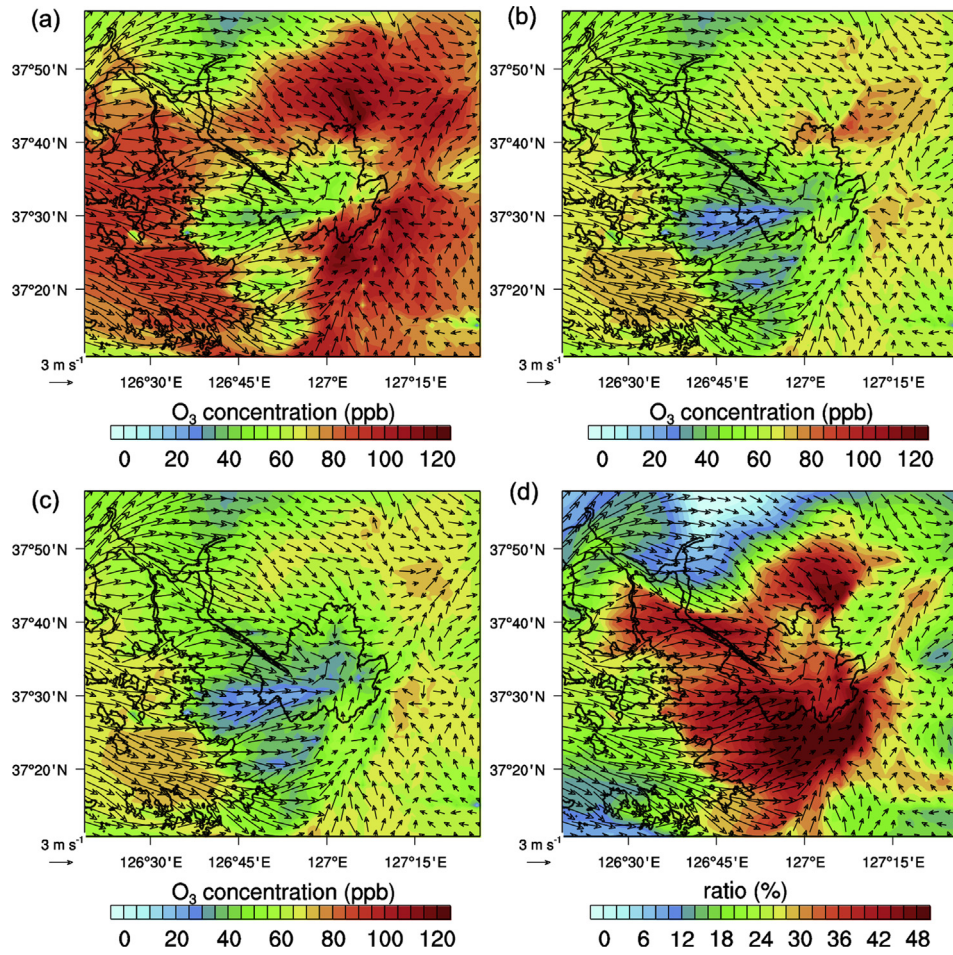


Fig. 5. Near-surface O₃ concentration and horizontal wind fields at 1600 LT in the (a) OUT, (b) IN, and (c) NONE simulations. (d) Field of the ratio (%) of the differences in near-surface O₃ concentration between the ALL and IN simulations to the near-surface O₃ concentration in the ALL simulation and the near-surface horizontal wind field at 1600 LT.

implemented in the CMAQ modeling system is performed, and the analysis results of the ALL, OUT, IN, and NONE simulations are compared. The IPR analysis quantifies the contributions of individual processes (e.g., advection, diffusion, deposition, and chemistry) to a concentration of each target species. Note that both horizontal and vertical components are integrated in the contributions of advection and diffusion processes. Fig. 6 shows the atmospheric boundary layer-averaged contributions of individual processes to O₃ concentration in the Seoul region from 0600 to 2000 LT. In the ALL simulation (Fig. 6a), the most important process for increasing O₃ concentration is the diffusion process until 1000 LT, the chemistry process from 1100 to 1600 LT, and the advection process after 1700 LT. The averaged contribution of chemistry process from 1100 to 1600 LT is 6.1 ppb h⁻¹. In addition to the increase due to photochemical production in the daytime, the O₃ concentration increases due to diffusion through the top of the atmospheric boundary layer in the morning and advection from the surrounding region in the late afternoon and evening. The contribution of deposition process to O₃ concentration is negligible because of the small dry deposition velocity of O₃ under a dry weather condition. The temporal variations of the contributions of individual processes in the OUT, IN, and NONE simulations are similar to those in the ALL simulation (Fig. 6b–d). Whereas the contributions of diffusion and advection processes in the OUT, IN, and NONE simulations are relatively unchanged, the contributions of chemistry process in the OUT, IN, and NONE simulations are not

as large as that in the ALL simulation in the daytime, which are 3.7, 2.4, and 0.5 ppb h⁻¹, respectively, when averaged from 1100 to 1600 LT. The contribution of chemistry process is the largest from 1100 to 1500 LT in the OUT simulation, from 1200 to 1500 LT in the IN simulation, and from 1300 to 1400 LT in the NONE simulation, the period in each simulation being shorter than that in the ALL simulation.

Fig. 7 shows the vertical profiles of the contributions of individual processes to O₃ concentration in the Seoul region averaged for the period from 1100 to 1600 LT. In the ALL simulation, O₃ is chemically produced throughout the atmospheric boundary layer except for the two lowest shallow layers, diffused down to the lower layers, and finally titrated with NO. To some extent, O₃ is advected from the surrounding region to the Seoul region in the lower part of the atmospheric boundary layer. The diffusion process from the upper layers down to the lower layers weakens in the IN and NONE simulations, while it is still effective in the OUT simulation. On the other hand, the advection process acts to move O₃ out of the Seoul region in the upper part of the atmospheric boundary layer in the IN and NONE simulations.

From the IPR analysis results, it is presumed that the dominant contributor to the increase in O₃ concentration in the Seoul region is not the advection of O₃ from the surrounding region into the Seoul region but the advection of one or more precursors into the Seoul region in the lower part of the atmospheric boundary layer followed by the chemical production in the atmospheric boundary

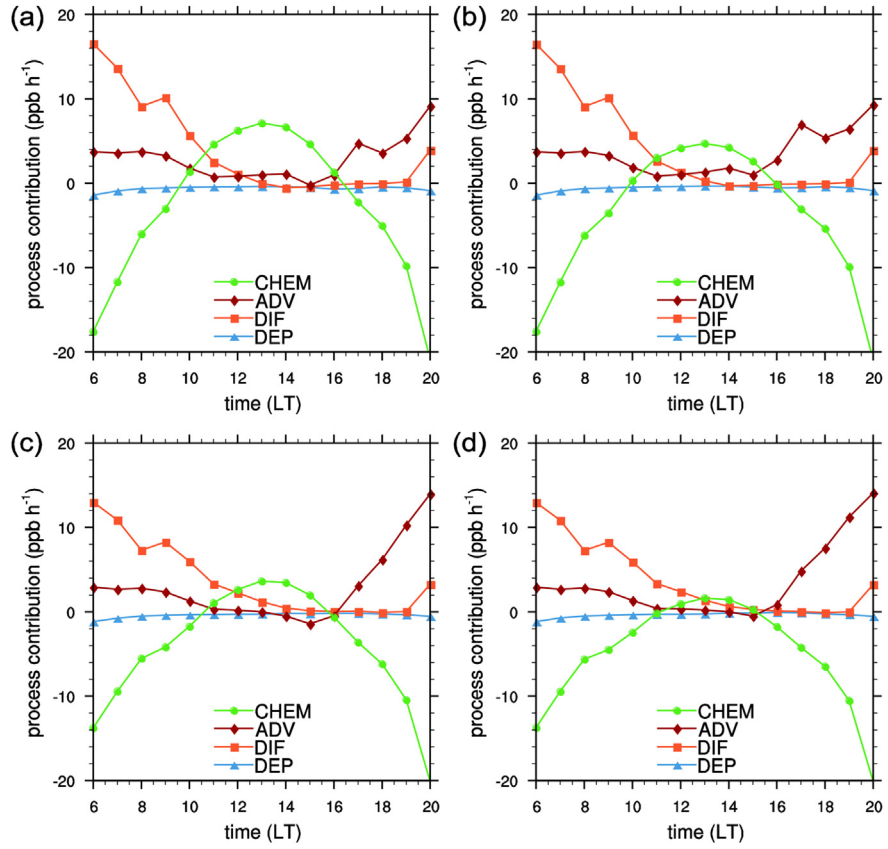


Fig. 6. Temporal variations of the atmospheric boundary layer-averaged contributions of individual processes to O₃ concentration in the Seoul region from 0600 to 2000 LT in the (a) ALL, (b) OUT, (c) IN, and (d) NONE simulations.

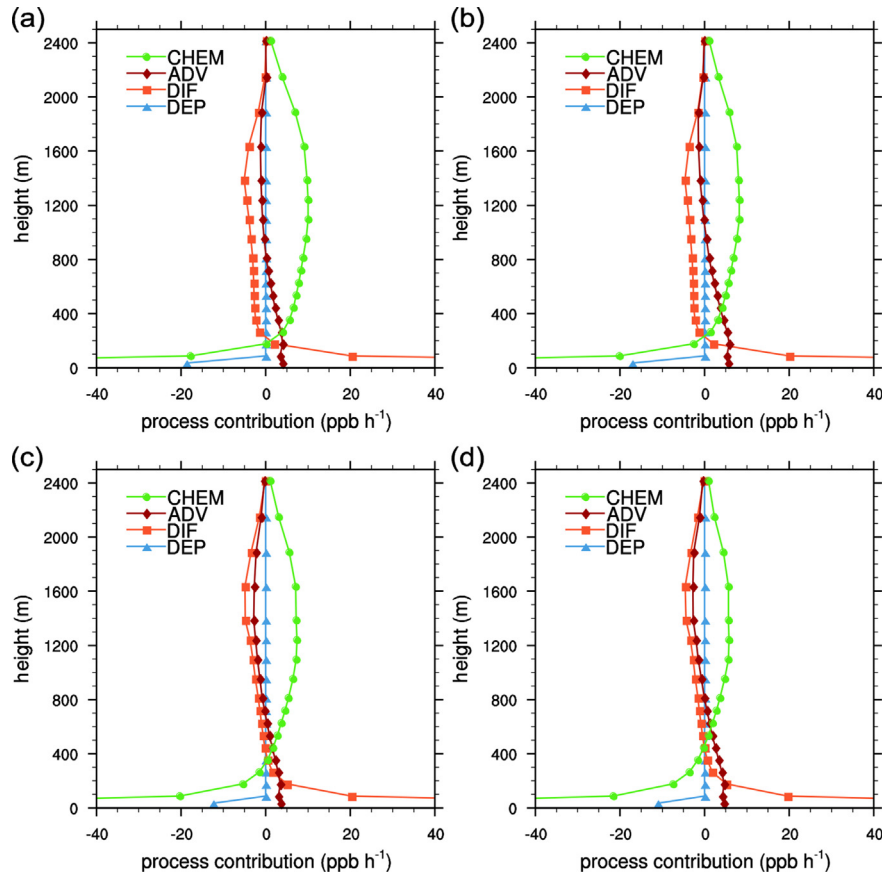
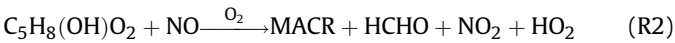
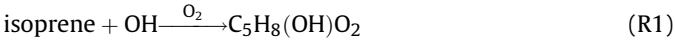


Fig. 7. 5-h averaged vertical profiles of the contributions of individual processes to O₃ concentration in the Seoul region for the period from 1100 to 1600 LT in the (a) ALL, (b) OUT, (c) IN, and (d) NONE simulations.

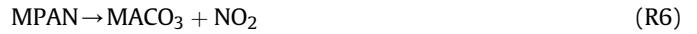
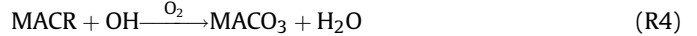
layer. As discussed in Fig. 4, isoprene is not a major precursor directly transported into the Seoul region. In the following subsection, we aim to look into which precursors oxidized from isoprene are responsible contributors to the increase in O₃ concentration in the Seoul region.

3.4. Roles of isoprene oxidation products

Isoprene, which has a chemical lifetime shorter than an hour, experiences sequential oxidation initiated by OH radical in the daytime (Paulson and Seinfeld, 1992).



The primary products of isoprene oxidation in reactions (R1)–(R3) are methacrolein (MACR), methyl vinyl ketone (MVK), and formaldehyde (HCHO). For example, Luecken et al. (2012) showed that the contribution of isoprene oxidation to HCHO concentration in summer spatially varies within a range of 20–60%. In addition, various types of aldehyde such as acetaldehyde (CCHO) and other aldehydes are secondary products in sequential isoprene oxidation processes. While a number of alkyl peroxy radicals (RO₂) are produced in sequential isoprene oxidation processes, peroxy-methacrylyl radical (MACO₃), which is one of RO₂, reacts with NO₂ to produce peroxy methacryloyl nitrate (MPAN) (Grosjean et al., 1993a, 1993b).



MPAN has a chemical lifetime of approximately a few hours to 15 h. The chemical loss of MPAN is mainly due to the thermal decomposition and partly due to reactions with OH and O₃.

Many observational studies have mentioned that isoprene oxidation products such as MACR, MVK, and HCHO significantly participate in O₃ formation in the presence of sufficient NO_x (Biesenthal et al., 1997; Duane et al., 2002; Pang et al., 2009). Stroud et al. (2001) conducted a field measurement at an urban forested site in Nashville, USA, and stated that isoprene oxidation initiated by OH radical significantly occurs on the timescale of transport from the forest areas to the urban areas. Geng et al. (2011) performed regional air quality simulations for the major forests and the city of Shanghai, China, and suggested that carbonyls such as HCHO and CCHO produced by the continuous isoprene oxidation in forest areas play important roles in enhancing O₃ formation in urban areas. In addition to the oxidation products mentioned above, some previous studies have stated that MPAN is a useful indicator for estimating biogenic influences on local O₃ formation rather than long-range transport (Williams et al., 1997; Nouaime et al., 1998). MACO₃, which is produced by the thermal decomposition of MPAN, reacts with NO instead of NO₂ and then successively produces sufficient amounts of peroxy radicals that strongly participate in O₃ formation (LaFranchi et al., 2009). To examine important precursors contributing to the increase in O₃ concentration in urban areas,

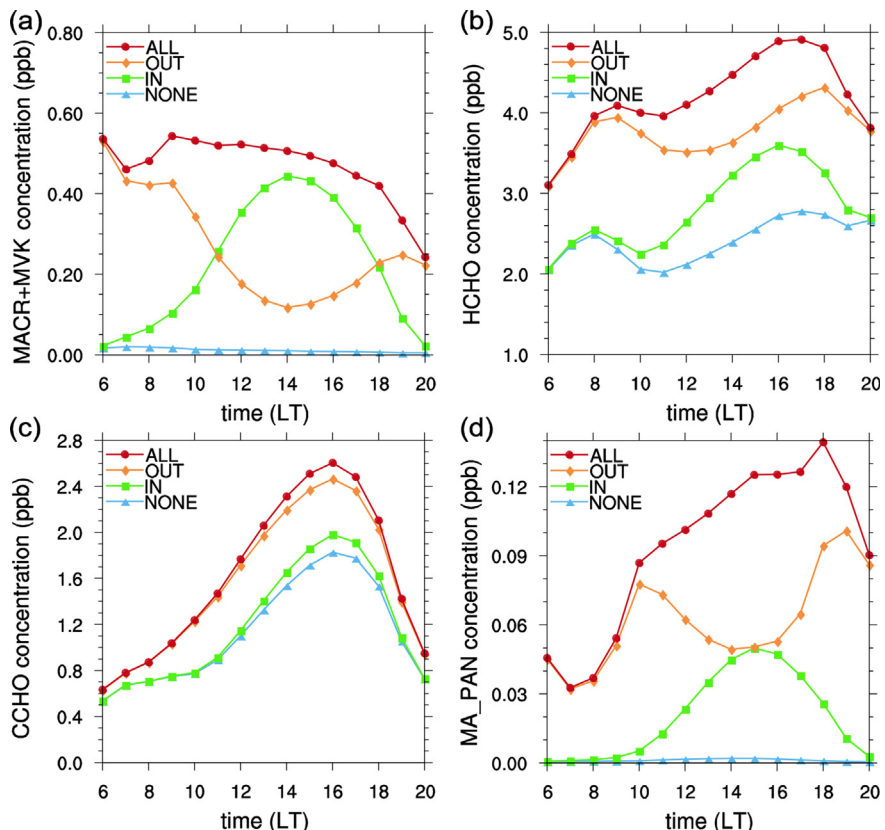


Fig. 8. Temporal variations of the atmospheric boundary layer-averaged (a) MACR + MVK, (b) HCHO, (c) CCHO, and (d) MA_PAN concentrations in the Seoul region from 0600 to 2000 LT in the ALL, OUT, IN, and NONE simulations.

MPAN in line with other oxidation products is also taken into account in this study.

The temporal variations of the atmospheric boundary layer-averaged MACR + MVK, HCHO, CCHO, MA_PAN concentrations in the ALL, OUT, IN, and NONE simulations are shown in Fig. 8. Note that MPAN is speciated by MA_PAN (a PAN analogue formed from MACR and other acroleins) in the SAPRC-99 chemical mechanism used in this study. The MACR + MVK concentration continuously decreases after 0900 LT in the ALL simulation. In the daytime, the MACR + MVK concentration is significantly higher in the IN simulation than in the OUT simulation because MACR and MVK are primary products of isoprene oxidation initiated by OH radical. The HCHO concentration is maximized at 1700 LT in the ALL simulation later than in the IN simulation and shows a relatively large sensitivity to the biogenic isoprene emission. On the other hand, the CCHO concentration is maximized consistently at 1600 LT in every simulation and shows a relatively small sensitivity to the biogenic isoprene emission because of a large portion of anthropogenic CCHO emission. The non-negligible HCHO and CCHO concentrations in the NONE simulation indicate significant contributions of other sources. The MA_PAN concentration is maximized at 1800 LT in coincidence with the O₃ concentration in the ALL simulation. The MA_PAN concentration shows a clear sensitivity to the biogenic isoprene emission. While the MA_PAN concentration in the NONE simulation is negligible compared to that in the other simulations, it is always higher in the OUT simulation than in the IN simulation.

Fig. 9 shows the near-surface concentration difference fields of MACR + MVK, HCHO, CCHO, and MA_PAN between the ALL and IN simulations and horizontal wind fields at 1600 LT. The positive values of concentration differences denote the increases in concentration due to the biogenic isoprene emission from the surrounding region. The influence of biogenic isoprene emission from the surrounding region is remarkable not only in the surrounding region but also in the Seoul region at 1600 LT. The isoprene oxidation products are largely produced in the surrounding region and transported into the Seoul region by the daytime local circulations that are well developed in the afternoon. The increase in MACR + MVK concentration in the Seoul region due to the biogenic isoprene emission from the surrounding region is shown to be limited in the Seoul region because of its rapid oxidation into other secondary products. The increases in HCHO and CCHO concentrations in the Seoul region due to the biogenic isoprene emission from the surrounding region are apparent. At 1600 LT, the prevailing westerly wind assists HCHO and CCHO to be transported into the Seoul region. On the other hand, the increase in MA_PAN concentration is affected by converging winds from the north and south. When the prevailing westerly wind passes by, MA_PAN is significantly swept out of the Seoul region to the east.

Fig. 10 shows the 5-h averaged vertical profiles of the contribution differences of individual processes to MACR + MVK, HCHO, CCHO, and MA_PAN concentrations between the ALL and IN simulations in the Seoul region for the period from 1100 to 1600 LT. In the lower part of the atmospheric boundary layer, MACR + MVK

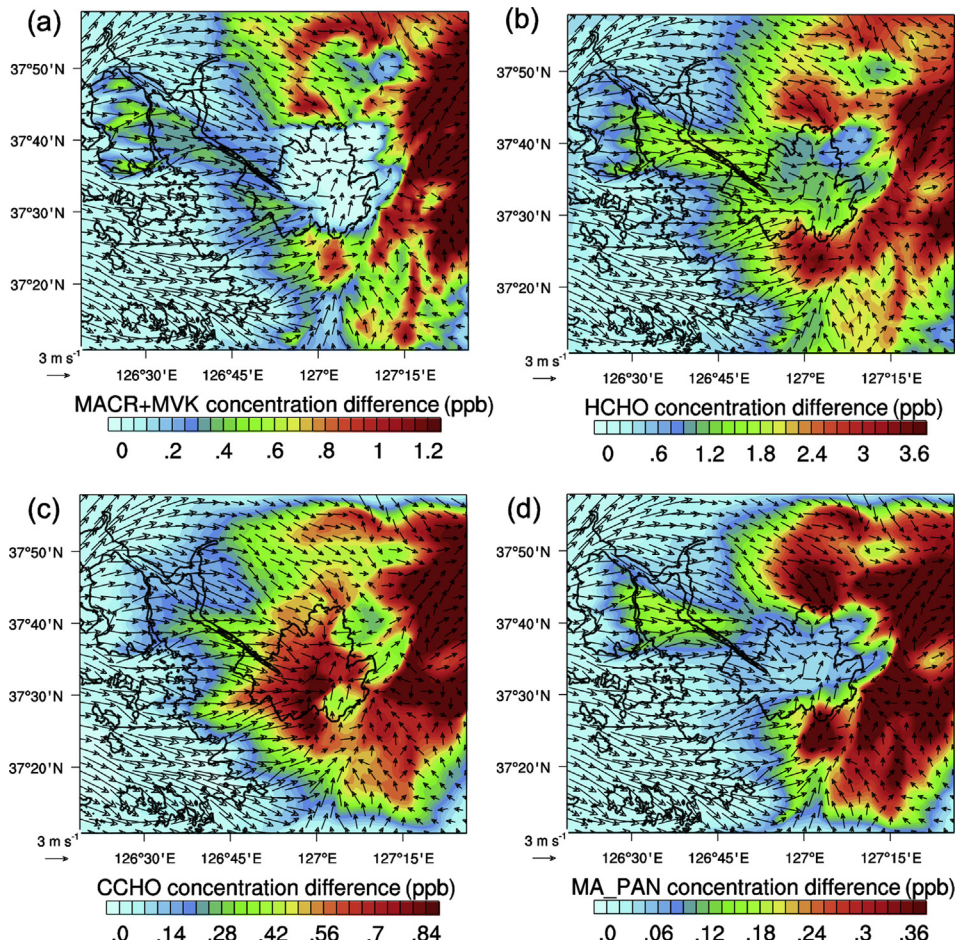


Fig. 9. Near-surface concentration difference (ALL–IN) fields of (a) MACR + MVK, (b) HCHO, (c) CCHO, and (d) MA_PAN between the ALL and IN simulations and horizontal wind fields at 1600 LT.

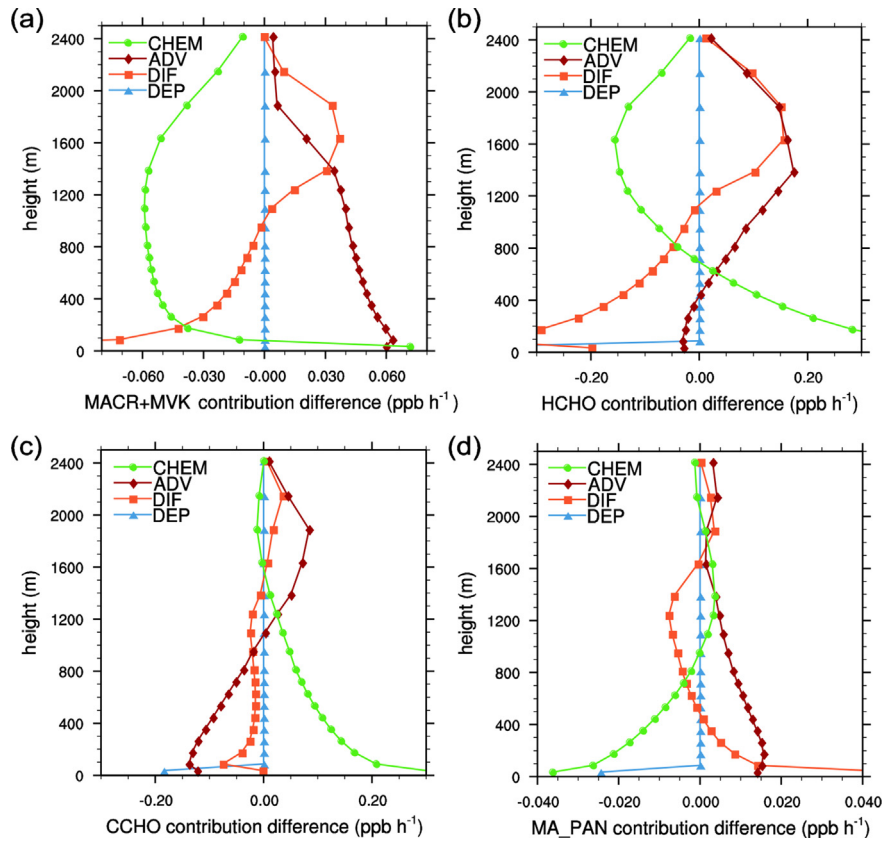


Fig. 10. 5-h averaged vertical profiles of the contribution differences (ALL-IN) of individual processes to (a) MACR + MVK, (b) HCHO, (c) CCHO, and (d) MA_PAN concentrations between the ALL and IN simulations in the Seoul region for the period from 1100 to 1600 LT.

and MA_PAN are transported from the surrounding region to the Seoul region. HCHO and CCHO transported from the surrounding region to the Seoul region are significantly converged and then vertically transported to the upper part at the convergence zones. As discussed in Fig. 9, this is associated with the different pathways dominantly from the westerly wind for HCHO and CCHO, and northerly and southerly winds for MA_PAN. The significant chemical losses of MACR + MVK throughout the atmospheric boundary layer except for the lowest shallow layer due to the isoprene emission indicate continuous oxidation mainly by OH into other secondary products enriching peroxy radicals (i.e., HO₂ and RO₂) in the Seoul region. In addition to transport by the local circulations, HCHO and CCHO are continuously produced as the secondary products in the lower part of the atmospheric boundary layer when the photolysis of HCHO and CCHO produces HO₂ in the daytime. After transported, MA_PAN is chemically decomposed into MACO₃ and NO₂ in the lower part of the atmospheric boundary layer. The isoprene oxidation products enrich peroxy radicals in the Seoul region where peroxy radicals dominantly react with NO to produce NO₂ in the presence of sufficient NO_x (Archibald et al., 2010). As a result, the transported isoprene oxidation products contribute to O₃ formation in the lower part of the atmospheric boundary layer.

4. Summary and conclusions

The impacts of biogenic isoprene emission on O₃ concentration in the SMA were investigated using the CMAQ modeling system coupled with the WRF model. The daily maximum O₃ concentration averaged over the Seoul region increases by 37 ppb due to the biogenic isoprene emission for this case. The biogenic isoprene

emission from the surrounding region has a greater influence on the O₃ concentration in the Seoul region than that from within the Seoul region. In addition, the biogenic isoprene emission from the surrounding region tends to delay the appearance of a daily maximum O₃ concentration. Isoprene oxidation products (MACR, MVK, HCHO, CCHO, and MA_PAN) are examined as important precursors for increasing O₃ concentration in the Seoul region. The precursors produced by sequential isoprene oxidation processes are transported from the surrounding region into the Seoul region by the daytime local circulations. While the effect of MACR and MVK transport is limited due to their rapid oxidation into secondary products, aldehydes (HCHO and CCHO) and MA_PAN are transported into the Seoul region dominantly by daytime local circulations. These are important pathways that the biogenic isoprene emission from the surrounding region increases the O₃ concentration in the Seoul region in the daytime.

This study demonstrates that the impacts of biogenic isoprene emission from the surrounding region on O₃ concentration in the Seoul region are evidently large in the afternoon. This study investigated a summer case when the well-developed local circulation enables the significant transport effect. The significance of oxidation product roles on local O₃ air quality in urban areas might depend on local meteorology. Thus, further studies are required for consolidated conclusions.

Acknowledgments

The authors are grateful to two anonymous reviewers for providing valuable comments that led to the improvements of the original manuscript. This work was supported by the National

Research Foundation of Korea (NRF) grant funded by the Korea Ministry of Science, ICT and Future Planning (MSIP) (No. 2011–0017041).

References

- Archibald, A.T., Jenkin, M.E., Shallcross, D.E., 2010. An isoprene mechanism inter-comparison. *Atmos. Environ.* 44, 5356–5364.
- Biesenthal, T.A., Wu, Q., Shepson, P.B., Wiebe, H.A., Anlauf, K.G., Mackay, G.I., 1997. A study of relationships between isoprene, its oxidation products, and ozone, in the Lower Fraser Valley, BC. *Atmos. Environ.* 31, 2049–2058.
- Byun, D., Schere, K.L., 2006. Review of the governing equations, computational algorithms, and other components of the models-3 community multiscale air quality (CMAQ) modeling system. *Appl. Mech. Rev.* 59, 51–77.
- Carter, W.P.L., 2000. Documentation of the SAPRC-99 Chemical Mechanism for VOC Reactivity Assessment. Final Report to California Air Resources Board, Contract No. 92–329 and 95–308.
- Chameides, W.L., Lindsay, R.W., Richardson, J., Kiang, C.S., 1988. The role of biogenic hydrocarbons in urban photochemical smog: Atlanta as a case study. *Science* 241, 1473–1475.
- Chang, C.-C., Chen, T.-Y., Lin, C.-Y., Yuan, C.-S., Liu, S.-C., 2005. Effects of reactive hydrocarbons on ozone formation in southern Taiwan. *Atmos. Environ.* 39, 2867–2878.
- Duan, J., Tan, J., Yang, L., Wu, S., Hao, J., 2008. Concentration, sources and ozone formation potential of volatile organic compounds (VOCs) during ozone episode in Beijing. *Atmos. Res.* 88, 25–35.
- Duane, M., Poma, B., Rembges, D., Astorga, C., Larsen, B.R., 2002. Isoprene and its degradation products as strong ozone precursors in Insubria, Northern Italy. *Atmos. Environ.* 36, 3867–3879.
- Foley, K.M., Roselle, S.J., Appel, K.W., Bhave, P.V., Pleim, J.E., Otte, T.L., Mathur, R., Sarwar, G., Young, J.O., Gilliam, R.C., Nolte, C.G., Kelly, J.T., Gilliland, A.B., Bash, J.O., 2010. Incremental testing of the community multiscale air quality (CMAQ) modeling system version 4.7. *Geosci. Model Dev.* 3, 205–226.
- Geng, F., Tie, X., Guenther, A., Li, G., Cao, J., Harley, P., 2011. Effect of isoprene emissions from major forests on ozone formation in the city of Shanghai, China. *Atmos. Chem. Phys.* 11, 10449–10459.
- Ghim, Y.S., Oh, H.S., Chang, Y.-S., 2001. Meteorological effects on the evolution of high ozone episodes in the greater Seoul area. *J. Air Waste Manag. Assoc.* 51, 185–202.
- Grosjean, D., Williams II, E.L., Grosjean, E., 1993a. Gas phase reaction of the hydroxyl radical with the unsaturated peroxyacetyl nitrate $\text{CH}_2=\text{C}(\text{CH}_3)\text{C}(\text{O})\text{ONO}_2$. *Int. J. Chem. Kinet.* 25, 921–929.
- Grosjean, D., Grosjean, E., Williams II, E.L., 1993b. The reaction of ozone with MPAN, $\text{CH}_2=\text{C}(\text{CH}_3)\text{C}(\text{O})\text{ONO}_2$. *Environ. Sci. Technol.* 27, 2548–2552.
- Guenther, A., Karl, T., Harley, P., Wiedinmyer, C., Palmer, P.I., Geron, C., 2006. Estimates of global terrestrial isoprene emissions using MEGAN (model of emissions of gases and aerosols from nature). *Atmos. Chem. Phys.* 6, 3181–3210.
- Haagen-Smit, A.J., Fox, M.M., 1954. Photochemical ozone formation with hydrocarbons and automobile exhaust. *J. Air Pollut. Control Assoc.* 4, 105–109.
- Houyoux, M.R., Vukovich, J.M., Coats Jr., C.J., Wheeler, N.J.M., Kasibhatla, P.S., 2000. Emission inventory development and processing for the seasonal model for regional air quality (SMRAQ) project. *J. Geophys. Res.* 105, 9079–9090.
- Jeffries, H.E., Tonnesen, S., 1994. A comparison of two photochemical reaction mechanisms using mass balance and process analysis. *Atmos. Environ.* 28, 2991–3003.
- Jeon, W.-B., Lee, S.-H., Lee, H.-W., Kim, H.-G., 2012. Process analysis of the impact of atmospheric recirculation on consecutive high- O_3 episodes over the Seoul Metropolitan Area in the Korean Peninsula. *Atmos. Environ.* 63, 213–222.
- LaFranchi, B.W., Wolfe, G.M., Thornton, J.A., Harrold, S.A., Browne, E.C., Min, K.E., Wooldridge, P.J., Gilman, J.B., Kuster, W.C., Goldan, P.D., de Gouw, J.A., McKay, M., Goldstein, A.H., Ren, X., Mao, J., Cohen, R.C., 2009. Closing the peroxy acetyl nitrate budget: observations of acyl peroxy nitrates (PAN, PPN, and MPAN) during BEARPEX 2007. *Atmos. Chem. Phys.* 9, 7623–7641.
- Lee, D.S., Holland, M.R., Falla, N., 1996. The potential impact of ozone on materials in the U.K. *Atmos. Environ.* 30, 1053–1065.
- Li, G., Zhang, R., Fan, J., Tie, X., 2007. Impacts of biogenic emissions on photochemical ozone production in Houston, Texas. *J. Geophys. Res.* 112, D10309. <http://dx.doi.org/10.1029/2006JD007924>.
- Lin, S., Liu, X., Le, L.H., Hwang, S.-A., 2008. Chronic exposure to ambient ozone and asthma hospital admissions among children. *Environ. Health Perspect.* 116, 1725–1730.
- Luecken, D.J., Hutzell, W.T., Strum, M.L., Pouliot, G.A., 2012. Regional sources of atmospheric formaldehyde and acetaldehyde, and implications for atmospheric modeling. *Atmos. Environ.* 47, 477–490.
- McDonnell, W.F., Abbey, D.E., Nishino, N., Lebowitz, M.D., 1999. Long-term ambient ozone concentration and the incidence of asthma in nonsmoking adults: the ahsmog study. *Environ. Res. Sect. A* 80, 110–121.
- Milford, J.B., Russell, A.G., McRae, G.J., 1989. A new approach to photochemical pollution control: implications of spatial patterns in pollutant responses to reductions in nitrogen oxides and reactive organic gas emissions. *Environ. Sci. Technol.* 23, 1290–1301.
- Milford, J.B., Gao, D., Sillman, S., Blossey, P., Russell, A.G., 1994. Total reactive nitrogen (NO_y) as an indicator of the sensitivity of ozone to reductions in hydrocarbon and NO_x emissions. *J. Geophys. Res.* 99, 3533–3542.
- Nouaime, G., Bertman, S.B., Seaver, C., Elyea, D., Huang, H., Shepson, P.B., Starn, T.K., Riemer, D.D., Zika, R.G., Olszyna, K., 1998. Sequential oxidation products from tropospheric isoprene chemistry: MACK and MPAN at a NO_x -rich forest environment in the southeastern United States. *J. Geophys. Res.* 103, 22463–22471.
- Pang, X., Mu, Y., Zhang, Y., Lee, X., Yuan, J., 2009. Contribution of isoprene to formaldehyde and ozone formation based on its oxidation products measurement in Beijing, China. *Atmos. Environ.* 43, 2142–2147.
- Park, C., Schade, G.W., Boedeker, I., 2011. Characteristics of the flux of isoprene and its oxidation products in an urban area. *J. Geophys. Res.* 116, D21303. <http://dx.doi.org/10.1029/2011JD015856>.
- Paulson, S.E., Seinfeld, J.H., 1992. Development and evaluation of a photooxidation mechanism for isoprene. *J. Geophys. Res.* 97, 20703–20715.
- Ryu, Y.-H., Baik, J.-J., Lee, S.-H., 2011. A new single-layer urban canopy model for use in mesoscale atmospheric models. *J. Appl. Meteorol. Climatol.* 50, 1773–1794.
- Ryu, Y.-H., Baik, J.-J., Kwak, K.-H., Kim, S., Moon, N., 2013. Impacts of urban land-surface forcing on ozone air quality in the Seoul metropolitan area. *Atmos. Chem. Phys.* 13, 2177–2194.
- Ryu, Y.-H., Baik, J.-J., 2013. Daytime local circulations and their interactions in the Seoul metropolitan area. *J. Appl. Meteorol. Climatol.* 52, 784–801.
- Shin, H.J., Kim, J.C., Lee, S.J., Kim, Y.P., 2013. Evaluation of the optimum volatile organic compounds control strategy considering the formation of ozone and secondary organic aerosol in Seoul, Korea. *Environ. Sci. Pollut. Res.* 20, 1468–1481.
- Sillman, S., 1999. The relation between ozone, NO_x , and hydrocarbons in urban and polluted rural environment. *Atmos. Environ.* 33, 1821–1845.
- Skamarock, W.C., Klemp, J.B., Dudhia, J., Gill, D.O., Barker, D.M., Duda, M.G., Huang, X.-Y., Wang, W., Powers, J.G., 2008. A Description of Advanced Research WRF Version 3. NCAR Technical Note NCAR/TN-475+STR.
- Stroud, C.A., Roberts, J.M., Goldan, P.D., Kuster, W.C., Murphy, P.C., Williams, E.J., Hereid, D., Parrish, D., Sueper, D., Trainer, M., Fehsenfeld, F.C., Apel, E.C., Riemer, D., Wert, B., Henry, B., Fried, A., Martinez-Harder, M., Harder, H., Brune, W.H., Li, G., Xie, H., Young, V.L., 2001. Isoprene and its oxidation products, methacrolein and methylvinyl ketone, at an urban forested site during the 1999 Southern Oxidants Study. *J. Geophys. Res.* 106, 8035–8046.
- Trahan, N.A., Peterson, C.M., 2007. Factors Impacting the Health of Roadside Vegetation. Final Report No. CDOT-DTD-R-2005-12.
- Williams, J., Roberts, J.M., Fehsenfeld, F.C., Bertman, S.B., Buhr, M.P., Goldan, P.D., Hübler, G., Kuster, W.C., Ryerson, T.B., Trainer, M., Young, V., 1997. Regional ozone from biogenic hydrocarbons deduced from airborne measurements of PAN, PPN, and MPAN. *Geophys. Res. Lett.* 24, 1099–1102.
- World Health Organization (WHO), 13–15 January 2003. Health Aspects of Air Pollution with Particulate Matter, Ozone and Nitrogen Dioxide. Report on a WHO working group; Bonn, Germany. EUR/03/5042688. Available at: <http://www.euro.who.int/document/e79097.pdf>.